

Single-shot measurement of triplet-singlet relaxation in a Si/SiGe double quantum dot

J. R. Prance,¹ Zhan Shi,¹ C. B. Simmons,¹ D. E. Savage,¹ M. G. Lagally,¹ L. R. Schreiber,² L. M. K. Vandersypen,² Mark Friesen,¹ Robert Joynt,¹ S. N. Coppersmith,¹ and M. A. Eriksson¹

¹University of Wisconsin-Madison, Madison, WI 53706

²Kavli Institute of Nanoscience, TU Delft, Lorentzweg 1, 2628 CJ Delft, The Netherlands

We investigate the lifetime of two-electron spin states in a few-electron Si/SiGe double dot. At the transition between the (1,1) and (0,2) charge occupations, Pauli spin blockade provides a readout mechanism for the spin state. We use the statistics of repeated single-shot measurements to extract the lifetimes of multiple states simultaneously. At zero magnetic field, we find that all three triplet states have equal lifetimes, as expected, and this time is ~ 10 ms. At non-zero field, the T_0 lifetime is unchanged, whereas the T_- lifetime increases monotonically with field, reaching 3 seconds at 1 T.

PACS numbers: 73.63.Kv, 85.35.Gv, 73.21.La, 73.23.Hk

The lifetimes of single electron spins in silicon have recently been measured to be as long as seconds in Si nanodevices, including gated quantum dots and donors [1–4], a promising step towards silicon spin qubits. Two-electron singlet-triplet states in a double dot can also be used as qubits [5–7], with the advantages that gating operations can be fast and that readout depends on the singlet-triplet energy splitting, which can be much larger than the single spin Zeeman energy at low magnetic fields. The lifetimes of singlet and triplet states have been measured in GaAs double dots and were found to depend on magnetic field, falling to $< 30 \mu\text{s}$ at zero field [8, 9]. In silicon, neither single-shot readout of the singlet-triplet qubit states, nor measurement of their lifetimes has been achieved up until now.

Here we report measurements of the lifetimes of singlet and triplet states in a Si/SiGe double quantum dot at magnetic fields from 1 T to 0 T obtained using single-shot read-out. Using pulsed gate voltages, we repeatedly alternate the charge detuning so that it first favors the (1,1) charge state (one electron in each dot) and then the (0,2) charge state (two electrons in one of the dots.) Because of Pauli spin blockade, charge transitions to (0,2) will only occur when the spin state is a singlet. We perform hundreds of thousands of such cycles and measure the presence or absence of charge transitions using real-time charge sensing. By analyzing the statistics of such data, we characterize multiple relaxation processes simultaneously, in contrast to time-averaged measurements, which are only sensitive to the rate-limiting process. At zero magnetic field the triplet and singlet state lifetimes are between 5 and 25 ms, lifetimes that exceed those measured in GaAs by over two orders of magnitude. As magnetic field increases, the lifetime of the T_0 remains essentially constant, whereas the lifetime of the T_- increases dramatically, reaching 3 seconds at $B_{\parallel} = 1$ T. These long times are expected because of the small hyperfine coupling and spin-orbit interaction in Si quantum dots.

The device is fabricated on a phosphorus-doped

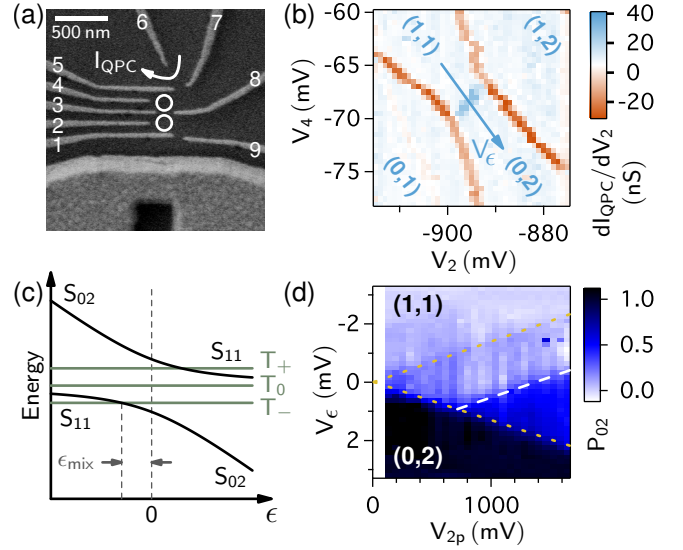


FIG. 1: (a) SEM image of a device identical to the one used. Quantum dots are formed at the approximate locations of the two circles. Charge sensing is performed by monitoring the current I_{QPC} through a nearby point-contact. (b) Charge stability diagram of the double dot showing the detuning voltage V_ϵ . (c) Energies of two-electron states as a function of detuning energy ϵ . T_+ , T_0 and T_- are the (1,1) triplets; the (0,2) triplets are higher in energy. The (1,1) and (0,2) singlets S_{11} and S_{02} are coupled by spin-preserving, inter-dot tunneling. A magnetic field separates the triplet energies by $E_z = g\mu_B B$. (d) Time-averaged occupation of the (0,2) charge state P_{02} at $B_{\parallel} = 0$ with 5 kHz square pulses applied along V_ϵ : pulse amplitudes on gates 2 and 4 are related by $V_{4p} = -0.35V_{2p}$. The pulses drive (1,1)-(0,2) transitions within the dotted triangle. The suppression of P_{02} above the dashed line shows where (1,1) to (0,2) tunneling is suppressed by spin blockade.

Si/Si_{0.7}Ge_{0.3} heterostructure with a strained Si quantum well approximately 75 nm below the surface. Palladium surface gates labelled 1-9 in Fig. 1(a) are used to form the double-dot confinement potential [10]. A thick RF antenna (Ti/Au, 5 nm/305 nm) is also present near the dot gates, but is unused in this experiment. All gates are connected to room temperature voltage sources via cold

RC filters, which are at the measurement base temperature of ≈ 15 mK. Gates 2 and 4 are also AC coupled to coaxial lines, allowing them to be pulsed at frequencies between 100 Hz and 1 GHz. There is an attenuation of ≈ 50 dB between each gate and the pulse source (a Tektronix AFG3252.) Current through the device is measured with a room-temperature current preamplifier with a bandwidth ≈ 1 kHz.

Figure 1(b) shows a charge stability diagram in which the absolute occupation of the dots was found by emptying both dots and then counting electrons back in. Fig. 1(c) shows the predicted energies of the two-electron states near the (1,1)-(0,2) transition as a function of detuning energy ϵ , where the transition is at $\epsilon = 0$ [11]. The detuning energy is controlled by varying the voltages on gates 2 and 4 along V_ϵ , shown in Fig. 1(b). The inter-dot tunnel coupling t_c was measured by determining where the S_{11} and T_- states cross at finite $B_{||}$. This is shown as ϵ_{mix} in Fig. 1(c), and depends on both $B_{||}$ and the curvature of the avoided singlet crossing. Using this approach [6], we find $t_c = 2.8 \pm 0.3 \mu\text{eV}$ (677 ± 73 MHz.)

To measure the spin of a (1,1) state we pulse the system into a spin blockaded configuration [12–14], where the ground state of the system is S_{02} and the (0,2) triplet states are higher in energy than all of the (1,1) triplets: T_- , T_0 and T_+ . We characterize the parameters needed to reach this configuration by detecting spin blockade in the time-averaged measurement shown in Fig. 1(d). Square pulses at 5 kHz are applied along V_ϵ . The color scale in Fig. 1(d) shows the time-averaged probability P_{02} of finding the system in (0,2) as a function of pulse amplitude and offset along V_ϵ . When the pulse crosses the (1,1)-(0,2) transition, tunneling between charge states results in $0 < P_{02} < 1$. The region where this occurs is bounded by the dotted triangle in Fig. 1(d). Spin blockade occurs in the part of the pulse triangle that is above the dashed white line in Fig. 1(d). Here we see $0 < P_{02} < 0.5$, because the system is residing in (1,1) the majority of the time.

Spin blockade does not occur below the white dashed line in Fig. 1(d), resulting in $P_{02} \approx 0.5$. In this region the pulse amplitude exceeds the (0,2) singlet-triplet splitting energy E_{ST} , and the pulse offset is such that the (0,2) triplet states have lower energy than the (1,1) triplets. From the size of the blockaded region, and the conversion from detuning voltage V_ϵ to detuning energy ϵ ($\Delta\epsilon = \Delta V_\epsilon \cdot 0.0676 \text{ eV/V}$, see supplemental material below for details), we find $E_{ST} = 124 \pm 4 \mu\text{eV}$.

Figure 2(a) and (b) show single-shot initialization and readout of (1,1) singlet and triplet states using real-time measurement of the charge state while pulsing across the (1,1)-(0,2) transition. The system is initialized by starting from the ground state S_{02} at $0 < \epsilon < E_{ST}$. The occupation of S_{02} is verified by measuring the charge state: S_{02} is the only (0,2) state accessible at this detuning. We then pulse to $\epsilon < 0$ to transfer the prepared S_{02} to the

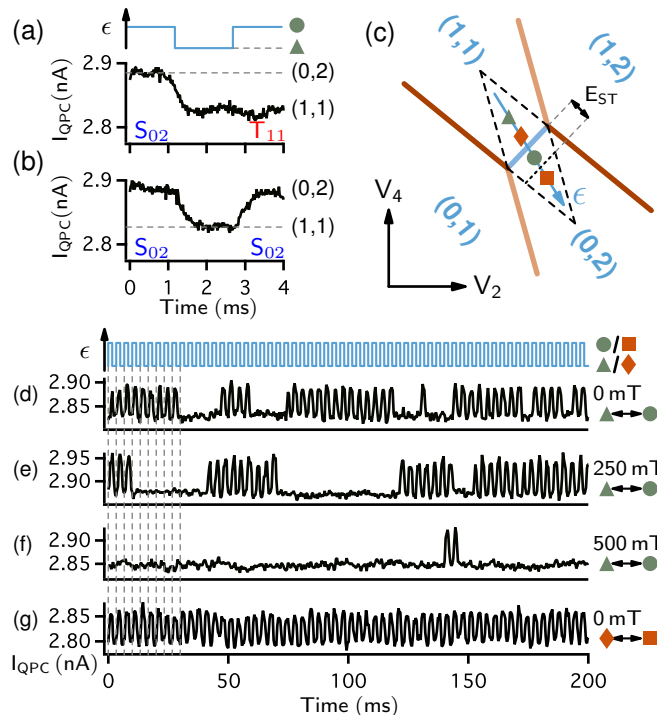


FIG. 2: Single-shot initialization and readout of singlet and triplet states. (a),(b) Real-time measurements of I_{QPC} as the system is initialized to S_{11} then read out 1.7 ms later. We identify the final state in (a) as one of the (1,1) triplets (T_{11}) because the (1,1) charge state survives for over 1 ms during the readout. In (b) a singlet is identified because the system tunnels quickly back to (0,2) during the readout. (c) Schematic stability diagram. The points marked are the four detuning values used in the measurements. At $B_{||} > 0$, E_{ST} is decreased by $g\mu_B B_{||}$. The pulse is offset to keep the circle inside the blockaded region without changing the separation of the circle and triangle points. Dashed triangles bound the region where (1,1)-(0,2) transitions occur primarily by inter-dot tunneling. (d)-(g) Pulses repeatedly switch the ground state between (1,1) and (0,2) at 300 Hz. In (d)-(f) the system is often blockaded in a (1,1) triplet. With increasing magnetic field from (d) to (f), the durations of blockade increase significantly. In (g), the pulse reaches into (0,2) far enough to exceed E_{ST} , and tunneling from (1,1) to (0,2) occurs freely for all spin states.

(1,1) singlet S_{11} . To measure the (1,1) spin state at some later time, we pulse back to $0 < \epsilon < E_{ST}$ where a singlet can tunnel quickly to (0,2) but the triplets cannot. The measurements are performed using detuning pulses with two levels that are at the positions of the filled triangle and circle in Fig. 2(c), which correspond to detuning energies of $\epsilon \approx -160 \mu\text{eV}$ and $60 \mu\text{eV}$ respectively at $B_{||} = 0$.

We measure the lifetimes of the (1,1) singlet and triplet states by detecting the spin state as we repeatedly pulse back and forth across the (1,1)-(0,2) transition at a frequency of 300 Hz. Fig. 2(d)-(f) show real-time measurements of the charge state as the pulses are applied. In this

regime spin blockade is active and the system switches randomly between free shuttling of a singlet state and blockade of a (1,1) triplet state. The typical length of time spent in a blocked triplet increases dramatically as B_{\parallel} increases. Fig 2(g) is a control, demonstrating that charge shuttles freely in both directions when the pulse is offset to reach outside the spin-blockade regime.

To determine the lifetimes of the states at $B_{\parallel} = 0$ we plot in Fig. 3(a) and (b) the number of times that blocked periods of duration t_b and un-blockaded periods of duration t_u are observed in 6.4 minutes of data (115,200 pulse periods). The histograms are very well fit by exponential decays, and fits to the two distributions give lifetimes of $\tau_b = 9.6 \pm 0.2$ ms for the blocked configuration and of $\tau_u = 23 \pm 3$ ms for the un-blockaded configuration. This shows that the lifetimes of the singlet and triplet states are ~ 10 ms.

The $B_{\parallel} = 0$ lifetimes are two orders of magnitude longer than have been seen in comparable low-field measurements of GaAs quantum dots [8, 9]. We suggest that this is due to the small hyperfine coupling in natural silicon, arising from the high abundance of zero-spin nuclei. At $B_{\parallel} = 0$, the (1,1) triplets are degenerate and separated from S_{11} by an energy $J(\epsilon) \approx t_c^2/\epsilon$. We expect singlet-triplet mixing to be driven by a small magnetic field difference between the two dots, resulting from the contact-hyperfine interaction with nuclear spins [15–17]. Predictions for the hyperfine coupling of (1,1) spin states are $h \sim 3$ neV in silicon [17], compared to measured values of $h \sim 50$ neV in GaAs [8, 18]. The expected coupling is small enough that, in our measurements, it would be exceeded by the exchange splitting J . Given t_c and the pulse amplitude, hyperfine induced singlet-triplet mixing should be suppressed by a factor of $(1 + (J/h)^2) \sim 500$, compared to the maximum mixing rate when $J \ll h$.

The values τ_u and τ_b show the time scale of singlet-triplet mixing, but they do not directly correspond to mixing times in any static configuration of the system. This is because the pulses continuously switch between two configurations, one at $\epsilon < 0$ and one at $\epsilon > 0$. The singlet-triplet mixing times may be different in the two configurations, and at $\epsilon > 0$ there are also fast, one-way transitions from S_{11} to S_{02} . We relate the measured values of τ_b and τ_u to singlet-triplet mixing times in the two configurations of the system by using rate equations to model state occupations during a single pulse cycle. The inputs to the model are two times; one time τ_- is the mixing time when the ground state is S_{11} during the $\epsilon < 0$ half of the pulse, and the other time τ_+ is the mixing time when the ground state is S_{02} during the $\epsilon > 0$ half of the pulse. Tunneling between S_{11} and S_{02} is assumed to be instantaneous. Mixing during the pulse transitions is ignored because the period of the pulse is 10^5 times larger than the pulse rise time. We solve for τ_+ and τ_- by numerical optimization of the model to match the measured values of τ_u and τ_b (see supplemental

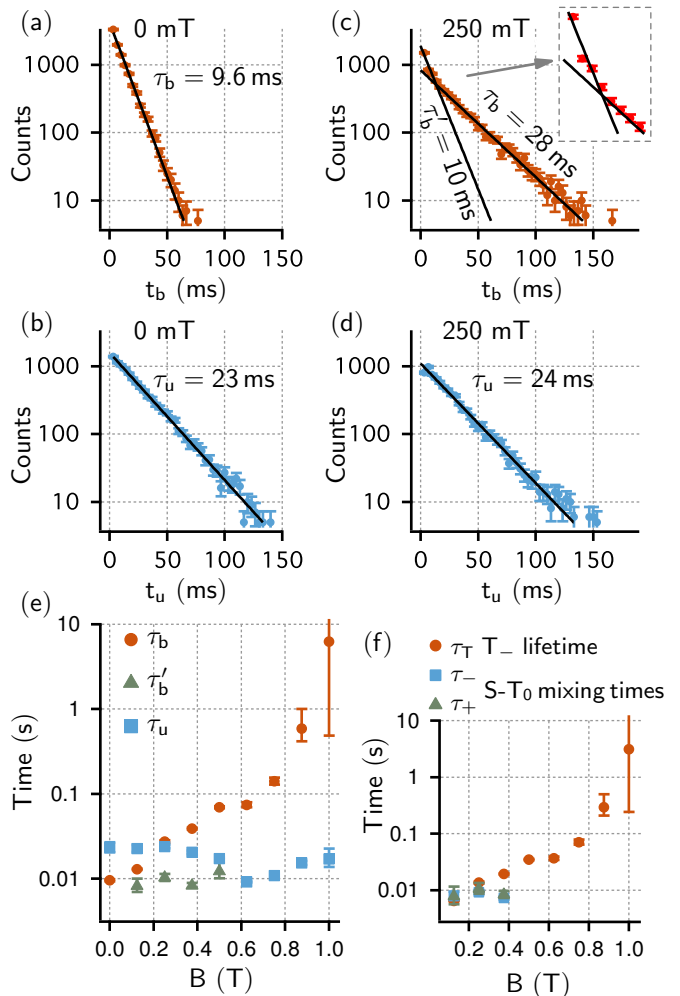


FIG. 3: Extracting lifetimes from real-time measurements. (a) Histogram of the number of times that the system is blocked for a time t_b in many measurements such as Fig. 2(d). The binning resolution is the pulse period. The solid line is an exponential fit yielding a lifetime for the blocked configuration of $\tau_b = 9.6$ ms. (b) Histogram of un-blockaded times (t_u) for the same data as (a). An exponential fit yields a lifetime for the un-blockaded configuration of $\tau_u = 23$ ms. (c), (d) Histograms of t_u and t_b at $B_{\parallel} = 250$ mT. There are two decay rates describing blockade: at small t_b there is a decay similar to that at zero field ($\tau'_b = 10$ ms). At long t_b a slower decay dominates ($\tau_b = 28$ ms). We interpret the shorter lifetime as that of the T_0 , and the longer lifetime as that of the T_- . (e) Fitted lifetimes as a function of magnetic field. The lifetime of blockade due to T_- states (τ_b) increases with field, while the contribution from T_0 and S_{11} states (τ'_b and τ_u) is field independent. (f) T_- lifetime τ_T , and S_{11} - T_0 mixing rate at positive (negative) detuning τ_+ (τ_-).

material below for details.) We find $\tau_- = 24.5 \pm 3$ ms and $\tau_+ = 5.8 \pm 0.3$ ms. We attribute the difference between τ_+ and τ_- to a difference in t_c between the two halves of each pulse cycle.

As B_{\parallel} increases from 0 T, we observe a qualitative change in the spin dynamics: the statistics of the block-

aded durations show two separate decay constants. As shown in Fig. 3(c) and (e), there are short blocked periods whose typical lifetime τ'_b is field independent, and there are longer blocked periods whose lifetime τ_b increases with field. The two lifetimes arise because the system can be blocked if it is in either a T_0 or a T_- state, and the T_- has a field dependent energy, whereas the T_0 does not. The T_+ state does not play a role at $B_{||} > 0$ because its higher energy means that it is rarely populated. Combined with statistics of un-blockaded durations, as in Fig. 3(d), each measurement at $B_{||} > 0$ can contain simultaneously information about the lifetimes of three states: the S_{11} , T_- and the T_0 .

Fig. 3(f) shows the T_- lifetime τ_T and S_{11} - T_0 mixing times τ_+ and τ_- calculated from the data in Fig. 3(e). We find τ_+ and τ_- from τ_u and τ'_b using a rate equation model similar to the zero field case, but with no transitions to T_+ and T_- included. This is because mixing from the S_{11} or T_0 to the T_+ and T_- will be suppressed due to their separation in energy. At $B_{||} \geq 0.5$ T, the system spends so much time in the T_- state that it is impractical to collect enough statistics to accurately determine τ'_b . Within the range of $B_{||}$ where τ'_b can be measured, the S_{11} - T_0 mixing rates are largely independent of field and similar to the rates seen at $B_{||} = 0$.

The time τ_T is the lifetime of the T_- during the $\epsilon > 0$ half of the pulse and is well approximated as $\tau_T = \tau_b/2$ at high magnetic field. During the $\epsilon < 0$ half of the pulse, T_- is the ground state and it will remain populated with high probability when $g\mu B_{||} > k_B T$. In the $\epsilon > 0$ half of the pulse the T_- is the first excited state and can decay to the S_{02} ground state at a rate τ_T^{-1} . Such transitions could be induced by phonons and a spin non-conserving process such as hyperfine coupling [8, 15, 16] or spin-orbit coupling [19–22]. We find that the T_- lifetime τ_T increases strongly with field, rising to 3 seconds by $B_{||} = 1$ T.

In summary, we have shown that we can initialize the singlet-triplet qubit state into a singlet and subsequently measure, in single-shot mode, transitions to the (1,1) triplet states. Using this initialization and real-time measurement, we have measured the lifetime of singlet and triplet states versus magnetic field. At zero magnetic field, the lifetime for the singlet and all three triplets is ~ 10 ms. At non-zero field, the T_0 and S_{11} lifetimes are almost unchanged, whereas the T_- lifetime grows significantly, reaching 3 seconds at 1T.

This work was supported by ARO and LPS (W911NF-08-1-0482) and by the United States Department of Defense. The US government requires publication of the following disclaimer: The views and conclusions contained in this document are those of the authors and should not be interpreted as representing the official policies, either expressly or implied, of the US Government. This research utilized NSF-supported shared facilities at the University of Wisconsin-Madison. LV acknowledges fi-

ancial support by a Starting Grant of the European Research Council (ERC) and by the Foundation for Fundamental Research on Matter (FOM).

SUPPLEMENTAL INFORMATION

Calibration of detuning energy

We find the conversion between detuning voltage V_ϵ and detuning energy ϵ by measuring the width of the (1,1)-(0,2) transition as a function of fridge temperature T_{fridge} . The relevant temperature scale for the double-dot system is the electron temperature T_e , which we model as

$$T_e = \sqrt{T_0^2 + T_{fridge}^2} \quad (1)$$

where T_0 is the base electron temperature of our measurement setup. In the limit where $k_B T_e$ is greater than the inter-dot tunnel coupling t_c , the width of the (1,1)-(0,2) transition will be determined by T_e . When $k_B T_e \ll t_c$, the width is independent of temperature [10, 23].

The line-shape of the inter-dot transition was measured by detecting the charge-sensor current I_{QPC} with a lock-in amplifier while gates 2 and 4 were swept across the transition in the direction V_ϵ (as shown in Fig. 1(b) of the main text): $\Delta V_2 = -1.375\Delta V_4$. The lock-in excitation was also applied in the V_ϵ direction by modulating gates 2 and 4 with a relative phase of 180 degrees and relative amplitudes of $V_{4p} = 0.35V_{2p}$. The excitation frequency was 500 Hz and the amplitude of the excitation at the gates was $\sim 20 \mu\text{V}$ on gate 4. The results were fit with the expected line-shape in the thermally broadened limit, which is the derivative of a Fermi function:

$$\frac{dI_{QPC}}{dV_\epsilon} = A \cosh^{-2} \left(\frac{\alpha(V_\epsilon - V_{\epsilon 0})}{2k_B T_e} \right) + C, \quad (2)$$

where the voltage changes along the detuning axis are given by $V_4 = V_\epsilon$ and $V_2 = -V_\epsilon/1.375$, and α is the conversion factor between V_ϵ and detuning energy.

Figure S1 shows the measured values of the transition width $k_B T_e / \alpha$ as a function of T_{fridge} . We find that the width depends on temperature down 50 mK, confirming our assumption that we are in the limit $k_B T_e > t_c$, and also indicating that the base electron temperature T_0 is < 50 mK. By fitting Equation 1 to the data, we find the calibration for the detuning energy to be $\alpha = 67.6 \text{ meV/V}$.

Zero magnetic field rate equation model

A set of coupled rate equations are used to extract S_{11} - T_0 mixing rates at zero magnetic field from the measured

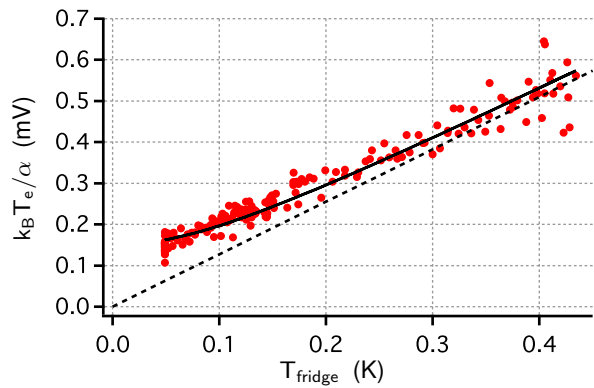


FIG. S1: Measured widths of the (1,1)-(0,2) transition as a function of the fridge temperature T_{fridge} . The solid line is a fit of the form given by Equation 1 with $T_0 = 10.3$ mK. The slope of the dependence at large temperatures yields the conversion between gate voltage along the detuning axis and energy: $\alpha = 67.6$ meV/V. The dotted line shows the conversion if T_0 is neglected, which agrees well with the data at large temperatures.

values τ_u and τ_b , which are the lifetimes of blockaded and un-blockaded configuration of the system. We relate τ_u and τ_b to the results of the rate equation model via two values: $P_R = e^{-T/\tau_u}$ is the probability of remaining un-blockaded in a single pulse cycle (the probability of returning to (0,2)), and $P_N = e^{-T/\tau_b}$ is the probability of remaining blockaded after a single pulse cycle (the probability of not returning to (0,2)). T is the period of the pulse cycle, which in all the experiments consists of two halves of equal duration. For the first half of the cycle ($t < T/2$), the system is at negative detuning ($\epsilon < 0$), which favors the (1,1) state, while during the second half of the cycle ($T/2 < t < T$), the system is at positive detuning, where the (0,2) state is favored.

The physical mechanisms we consider are inter-dot tunneling between S_{11} and S_{02} , and singlet-triplet mixing due to a small field difference between the dots arising from the hyperfine interaction with background nuclear spins. At zero external field, the time-averaged effect of the small field difference between the dots is to cause all the (1,1) triplet states to mix with the (1,1) singlet at the same rate [15, 16]. This mixing rate will depend on the singlet-triplet splitting $J \approx t_c^2/\epsilon$, where t_c is the inter-dot tunnel coupling and ϵ is the detuning energy. The two halves of each pulse cycle will have different values of $|\epsilon|$ and, possibly, slightly different values of t_c . We therefore allow for two singlet-triplet mixing rates for the two halves of the cycle.

The double-dot states included in the model are S_{11} , T_- , T_0 , T_+ and S_{02} , with occupation probabilities p_1 , p_2 , p_3 , p_4 and p_5 respectively. During the first half of the pulse cycle, while the system is at negative detuning ($\epsilon < 0$), we allow all three triplet states to mix with S_{11} at a rate ρ_- . The S_{02} state is assumed to be unpopulated

because it will quickly tunnel to S_{11} . The evolution of the occupation probabilities is given by:

$$\dot{p}_1(t) = \rho_- (p_2(t) + p_3(t) + p_4(t) - 3p_1(t)) \quad (3)$$

$$\dot{p}_2(t) = \rho_- (p_1(t) - p_2(t)) \quad (4)$$

$$\dot{p}_3(t) = \rho_- (p_1(t) - p_3(t)) \quad (5)$$

$$\dot{p}_4(t) = \rho_- (p_1(t) - p_4(t)) \quad (6)$$

$$\dot{p}_5(t) = 0 \quad (7)$$

During the second half of the pulse, from $t = T/2$ to $t = T$, the system is at positive detuning ($\epsilon > 0$) and the S_{02} is now the ground state. The rate of singlet-triplet mixing is ρ_+ , and we assume that all occupation of S_{11} is instantly transferred to S_{02} . The evolution of the occupation probabilities is given by:

$$\dot{p}_1(t) = 0 \quad (8)$$

$$\dot{p}_2(t) = -\rho_+ p_2(t) \quad (9)$$

$$\dot{p}_3(t) = -\rho_+ p_3(t) \quad (10)$$

$$\dot{p}_4(t) = -\rho_+ p_4(t) \quad (11)$$

$$\dot{p}_5(t) = \rho_+ (p_2(t) + p_3(t) + p_4(t)) \quad (12)$$

We note that the model yields the same results if transitions between triplets are also allowed.

The two sets of coupled rate equations, Eqn. 3-7 and Eqn. 8-12, are solved numerically to predict P_N and P_R for various ρ_- and ρ_+ . The values of ρ_- and ρ_+ are then optimized to best match P_N and P_R given by the measurements. Errors on ρ_- and ρ_+ are found by recalculating the model multiple times while varying P_N and P_R within a range given by the errors on τ_b and τ_u .

To calculate P_R , the initial conditions are set to unit probability of being in S_{11} : $p_1(0) = 1$ and $p_{N \neq 1}(0) = 0$. The occupation probabilities are evolved numerically for a time $T/2$ according to Eqn. 3-7. The resulting values of p_N are then used as initial conditions for a further evolution for time $T/2$ according to Eqn. 8-12; however, all occupation of S_{11} is first transferred to S_{02} to simulate the fast inter-dot tunnel coupling of these states. The probability of remaining un-blockaded for a single pulse period is then given by $P_R = p_5(T)$.

P_N is calculated in a similar way to P_R , but with the initial conditions being a unit probability of starting in a triplet state. The probability of remaining in a blockaded state for a single period is given by $P_N = \sum_{n=2}^4 p_n(T)$. Because of the symmetry of the rate equations, the answer is independent of which triplet is initially occupied.

The lifetimes found by experiment at zero magnetic field are $\tau_u = 23 \pm 3$ ms ($P_R = 0.87$) and $\tau_b = 9.6 \pm 0.2$ ms ($P_N = 0.71$). We find that these values are consistent with S_{11} - T_0 mixing times of $1/\rho_+ = 5.8 \pm 0.3$ ms and $1/\rho_- = 24.5 \pm 3$ ms.

-
- [1] M. Xiao, M. G. House, and H. W. Jiang, *Phys. Rev. Lett.* **104**, 096801 (2010).
- [2] A. Morello, et al., *Nature (London)* **467**, 687 (2010).
- [3] C. B. Simmons, J. R. Prance, B. J. Van Bael, T. S. Koh, Z. Shi, D. E. Savage, M. G. Lagally, R. Joynt, M. Friesen, S. N. Coppersmith, and M. A. Eriksson, *Phys. Rev. Lett.* **106**, 156804 (2011).
- [4] R. R. Hayes, et al., e-print arXiv:0908.0173 (2009).
- [5] J. Levy, *Phys. Rev. Lett.* **89**, 147902 (2002).
- [6] J. R. Petta, A. C. Johnson, J. M. Taylor, E. A. Laird, A. Yacoby, M. D. Lukin, C. M. Marcus, M. P. Hanson, and A. C. Gossard, *Science* **309**, 2180 (2005).
- [7] S. Foletti, H. Bluhm, D. Mahalu, V. Umansky, and A. Yacoby, *Nature Phys.* **5**, 903 (2009).
- [8] A. C. Johnson, J. R. Petta, J. M. Taylor, A. Yacoby, M. D. Lukin, C. M. Marcus, M. P. Hanson, and A. C. Gossard, *Nature (London)* **435**, 925 (2005).
- [9] J. R. Petta, A. C. Johnson, A. Yacoby, C. M. Marcus, M. P. Hanson, and A. C. Gossard, *Phys. Rev. B* **72**, 161301 (2005).
- [10] C. B. Simmons, M. Thalukulam, B. M. Rosemeyer, B. J. Van Bael, E. K. Sackmann, D. E. Savage, M. G. Lagally, R. Joynt, M. Friesen, S. N. Coppersmith, and M. A. Eriksson, *Nano Lett.* **9**, 3234 (2009).
- [11] R. Hanson, L. P. Kouwenhoven, J. R. Petta, S. Tarucha, and L. M. K. Vandersypen, *Rev. Mod. Phys.* **79**, 1217 (2007).
- [12] N. Shaji, et al., *Nature Phys.* **4**, 540 (2008).
- [13] M. G. Borselli, et al., *Appl. Phys. Lett.* **99**, 063109 (2011).
- [14] N. S. Lai, W. H. Lim, C. H. Yang, F. A. Zwanenburg, W. A. Coish, F. Qassemi, A. Morello, and A. S. Dzurak, e-print arXiv:1012.1410 (2010).
- [15] W. A. Coish and D. Loss, *Phys. Rev. B* **72**, 125337 (2005).
- [16] J. M. Taylor, J. R. Petta, A. C. Johnson, A. Yacoby, C. M. Marcus, and M. D. Lukin, *Phys. Rev. B* **76**, 035315 (2007).
- [17] L. V. C. Assali, H. M. Petrilli, R. B. Capaz, B. Koiller, X. Hu, and S. Das Sarma, *Phys. Rev. B* **83**, 165301 (2011).
- [18] F. H. L. Koppens, J. A. Folk, J. M. Elzerman, R. Hanson, L. H. Willems van Beveren, I. T. Vink, H. P. Tranitz, W. Wegscheider, L. P. Kouwenhoven, and L. M. K. Vandersypen, *Science* **309**, 1346 (2005).
- [19] C. Tahan, M. Friesen, and R. Joynt, *Phys. Rev. B* **66**, 035314 (2002).
- [20] M. Prada, R. H. Blick, and R. Joynt, *Phys. Rev. B* **77**, 115438 (2008).
- [21] M. Raith, P. Stano, and J. Fabian, *Phys. Rev. B* **83**, 195318 (2011).
- [22] L. Wang and M. W. Wu, *J. App. Phys.* **110**, 043716 (2011).
- [23] L. Dicarlo, H. J. Lynch, A. C. Johnson, L. I. Childress, K. Crockett, and C. M. Marcus, *Phys. Rev. Lett.* **92**, 226801 (2004).